UNIVERSIDAD NACIONAL AUTÓNOMA DE MEXICO
POSGRADO EN CIENCIAS FÍSICAS
INSTITUTO DE FÍSICA

STABLE DARK MATTER AND NEUTRINO MASSES FROM A DISCRETE GROUP

TESIS
QUE PARA OPTAR POR EL GRADO DE:
MAESTRO EN CIENCIAS (FÍSICA)

PRESENTA:
LEON MANUEL GARCIA DE LA VEGA

TUTOR PRINCIPAL
EDUARDO PEINADO RODRÍGUEZ
INSTITUTO DE FÍSICA UNAM

MIEMBROS DEL COMITÉ TUTOR
ERIC VÁZQUEZ JÁUREGUI
INSTITUTO DE FÍSICA UNAM
CESAR FERNANDEZ RAMIREZ
INSTITUTO DE CIENCIAS NUCLEARES UNAM

CIUDAD UNIVERSITARIA, CD. MX., AGOSTO 2019

Stable dark matter and neutrino masses from a discrete group

Leon Manuel Garcia de la Vega

May 2019

Acknowledgements

I thank and acknowledge the following financial supports

- DGAPA-PAPIIT IN107118
- DGAPA-PAPIIT IA102418
- German-Mexican Research Collaboration Grant No. SP 778/4-1 (DFG)
- Grant No. 278017 (CONACyT)
- CONACYT Postgraduate studies scholarship

Additionally I thank the College of William and Mary, the University of Colima and the International Center for Theoretical Physics for their hospitality.

Contents

Chapter 1

Introduction

The Standard Model (SM) of High Energy Physics is the most accurate model of fundamental interactions developed so far. Nevertheless several open questions in the area remain open. Two of the most compelling evidences for the incompleteness of the SM are neutrino oscillations and the astrophysical and cosmological observations of Dark Matter (DM). Both of these phenomenons can be solved by extending SM to include more particles and symmetries. The possibility that these two problems may be connected is intriguing.

1.1 Dark matter

To define what DM should be it would be useful to describe the observations that have led us to search for it. In 1933 the swiss astronomer Fritz Zwicky published a paper [1] where he uses the virial theorem to deduce the mass-to-light ratio of the Coma cluster. The result he obtained is that

> '...the average density in the Coma system would have to be at least 400 times greater than that derived on the basis of observations of luminous matter. ... If this should be verified, it would lead to the surprising result that dark matter exists in much greater density than luminous matter.' [1]

What this means is that the gravitational potential between the luminous matter in the cluster does not account for the velocity of galaxies in it. This is typically regarded as the first evidence for the existence of DM, and

[1] Translation from [2].

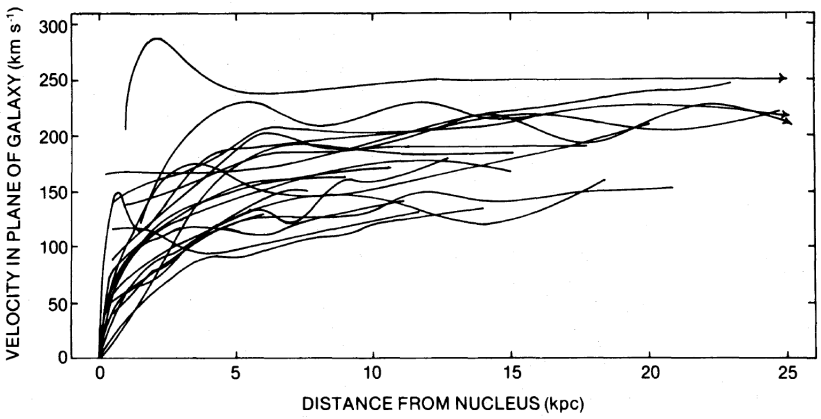

Figure 1.1: Rotation curves for 21 galaxies [3] . The horizontal axis shows the distance from the galactic radius in kiloparsecs and the vertical axis shows the velocity of gas on the galactic plane in $km\ s^{-1}$.

the first use of the term dark matter.
Several decades after Zwicky's observation, and shortly after the advent of radio astronomy, Vera Rubin observed a similar phenomenon on a smaller scale, in the rotation of gas inside cylindrically symetrical galaxies. According to Newtonian gravity (which should hold reasonably well for intragalactic motion) the speed v of this gas at a radius r from the center of the galaxy is

$$\mathrm{v}(r) = \sqrt{\frac{G_N M(r)}{r}}, \tag{1.1}$$

where G_N is the gravitational constant and $M(r)$ is the mass enclosed by a sphere of radius r. Rubin measured the speed of the rotating gas, by observing the Doppler shift of the hydrogen 21 cm line. The result is illustrated in Fig. (1.1). The expected behavior from the observed luminosity profile is a rise in $\mathrm{v}(r)$ in the central region from the rise in $M(r)$ in the dense center followed by a decline outside this region, where $M(r)$ changes insignificantly. The observed profile does not match this prediction, and instead shows a flat profile for large radiuses, suggesting the presence of nonluminous matter outside the bright center of galaxies.

Furthermore, weak lensing studies of colliding clusters in the Bullet system for example, show that there are non-emitting components of matter

that produce gravitational lensing of background sources. The studies consist of the mapping of matter distribution by X-ray emission and by weak lensing of background objects. X-ray mapping is sensitive to light-emitting gas and weak lensing is sensitive to all matter in the cluster. The disparity between these mappings proves the presence of non-emitting matter in the cluster, and its negligible friction with hydrogen gas and with itself [4].
Finally, the most successful model for describing the dynamics of the Universe, the Lambda-Cold Dark Matter (ΛCDM) model, predicts a DM to baryonic matter ratio of ~ 6. This ratio may be calculated by combining observations sensitive only to baryon density and comparing it to observations sensitive to all matter. There are several ways to measure the baryon density of the Universe, for example [5]

- By measuring the intensity of X-ray emission in groups of galaxies, where most of the baryons of the Universe are,
- By observing the absorption of light from distant sources by baryons along the line of sight,
- By analyzing the Cosmic Microwave Background (CMB), the relative height of the peaks of the anisotropy spectrum depends on baryon density,
- By measuring the abundance of light elements and comparing to predictions of Big Bang Nucleosynthesis.

All of these measurements are in good agreement with a cosmological density of baryons of

$$\Omega_b \sim 0.04, \tag{1.2}$$

with $\Omega_j \equiv \rho_j/\rho_{cr}$, where ρ_{cr} is the critical density of the Universe. On the other hand, to calculate the total matter density of the Universe Ω_m we rely on the following methods

- Weak lensing of distant light sources can quantify the matter density along the line of sight,
- The large scale structure of the Universe is mapped through galaxy surveys, its power spectrum depends on Ω_m through the cosmological model,
- The CMB anisotropy power spectrum depends too on Ω_m through ΛCDM, and it can determine Ω_m to $\sim 0.1\%$ accuracy,

among others. The matter density probes agree on a total matter density of $\Omega_m \sim 0.3$, leaving a gap of $\Omega_{CDM} \sim 0.25$ unaccounted for. This is what is called cold dark matter in cosmology.
From these and other observations we can infer some properties of DM, some of the most salient ones are

- Neutral - DM must not couple significantly with photons. Strong constraints on its charge and other electromagnetic form factors can be derived from astrophysical observations.

- Cold - DM must have cooled enough to form dense potential wells in the early universe to drive structure formation.

- Abundant - The production mechanism for DM in the early universe must produce enough abundance of DM particles to account for the observed Ω_m. It also need be stable, or very slowly decaying for this abundance not to drop from the structure formation era to today, and oversaturate the baryonic or radiation abundances.

In high energy physics many models of DM particles have been developed, but no experimental confirmation of any has been achieved. Among the many experimental probes of DM the most commonly cited ones are of three types: direct detection experiments, indirect detection experiments and collider production searches. Direct DM detection consists on the observation of a volume of a material called the target, waiting for a DM particle, from the local halo density, to interact with the nucleus of the target. Indirect detection consists in the observation of the spectrum of astroparticles, hoping to find a feature of the spectrum consistent with DM annihilation or decay. Collider searches consist on the production of DM in particle colliders, characterized by a missing energy signature in the outgoing particles. To date none of these searches have obtained strong signals to determine the properties of DM.
It should also be mentioned that the problem of DM has also been treated as a problem of general relativity, by assuming that the observations of ”excess gravity” in galaxies and clusters are the result of a modification of gravity, and not of an additional source of gravity. This class of theories are generically called Modified Newtonian Dynamics (MOND), and have been studied since the early 80’s [6]. Although they succeed in explaining galactic and cluster dynamics, they have faced problems when confronted with CMB data [7] or when confronted with cluster collision data [8].

1.2 Neutrino oscillations

The idea that neutrinos oscillate when propagating was first put forth by Pontecorvo in 1958 [9], based on a rumor that Davis had observed the lepton number violating process

$$\bar{\nu}_e + {}^{37}Cl \rightarrow e^- + {}^{37}Ar, \tag{1.3}$$

in a reactor experiment [10]. In Pontecorvo's paper he proposes neutrino-antineutrino mixing, in analogy to the $K^0 - \bar{K}^0$ system, to explain the obseration of such processes. After this work Pontecorvo proceeded to consider neutrino flavor mixing, in addition to mixing with sterile states. Although in the reactor neutrino experiment the anomaly disappeared, in solar neutrino observations Davis measured a third of the expected neutrino flux. This was called the solar neutrino problem, and was confirmed in directional detection experiments by Kamiokande during the 80's. Because these experiments are sensitive to high-energy neutrinos only (> 7 MeV), and the flux in the high energy region is highly sensitive to the solar model, it wasn't until the detection of this anomaly by GALLEX, which had a threshold of ~ 0.2 MeV, that the problem could be reasonably imputated to neutrino physics, rather than to solar physics. Similar discrepancies were observed in atmospheric neutrinos by IMB and Kamiokande. The oscillation of neutrinos was finally confirmed by experiments sensitive to the three neutrino flavors, and capable of discriminating between charged current and neutral current processes. This observation was made by SNO [11] and Kamiokande [12], finally measuring a total solar neutrino flux in good agreement with the Solar Standard Model. The existence of neutrino oscillations requires a mismatch between flavor and mass eigenstates, which means that neutrinos are massive particles. The origin of this mass and the mixing between states is an open problem, which cannot be solved within the SM of high energy physics. This is a reason to pursue the study of neutrinos, they provide a sure path to Beyond the SM (BSM) physics. In a further section of this work we shall explain some possible ways neutrinos can acquire mass and the potential phenomenology it implies.

Chapter 2

The Standard Model

2.1 Standard Model

The standard model of high energy Physics describes the matter content and interactions of all observed fundamental particles. It is based on the gauge group $G_{SM} = SU(3)_C \times SU(2)_L \times U(1)_Y$. The particle content can be classified in gauge bosons, quarks, leptons and the Higgs boson. The gauge bosons associated with the $SU(3)_C$ symmetry are the gluons G^i ($i = 1,..,8$), the bosons associated with $SU(2)_L$ are the W^j ($j = 1,2,3$), and the boson associated with $U(1)_Y$ is the B. The leptons are left-handed $SU(2)_L$ doublets L_α with hypercharge $Y_L = -1/2$ and right-handed $SU(2)_L$ singlets e_α with hypercharge $Y_e = -1$. Leptons are, characteristically, $SU(3)_C$ singlets. Quarks are left-handed $SU(2)_L$ doublets Q_α with hypercharge $Y_Q = 1/6$, right-handed $SU(2)_L$ singlets u_α with hypercharge $Y_u = 2/3$ and right-handed $SU(2)_L$ singlets d_α with hypercharge $Y_d = -1/3$. Quarks are $SU(3)_C$ triplets (quark color indices are suppressed in this text). For all quarks and leptons, there are 3 generations ($\alpha = 1,2,3$). Finally, the scalar Φ is an $SU(3)_C$ singlet, an $SU(2)_L$ doublet and it carries hypercharge $Y_\Phi = 1/2$. The particle content is summarized in Table (2.1).

The Lorentz and gauge invariant, renormalizable Lagrangian obtained is therefore

$$\mathscr{L}_{SM} = \mathscr{L}_g + \mathscr{L}_F + \mathscr{L}_\Phi + \mathscr{L}_Y, \tag{2.1}$$

where $\mathscr{L}_g$ is the gauge boson kinetic lagrangian, $\mathscr{L}_F$ is the fermion kinetic lagrangian, $\mathscr{L}_\Phi$ is the scalar lagrangian and $\mathscr{L}_Y$ is the Yukawa coupling lagrangian. The gauge bosons kinetic terms are

$$\mathscr{L}_g = -\frac{1}{4} G^\alpha_{\mu\nu} G^{\mu\nu\alpha} - \frac{1}{4} W^\alpha_{\mu\nu} W^{\mu\nu\alpha} - \frac{1}{4} B_{\mu\nu} B^{\mu\nu}, \tag{2.2}$$

Particle	Description	$SU(3)_C$	$SU(2)_L$	$U(1)_Y$
G^i	Gauge bosons	8	-	-
W^j	Gauge bosons	-	3	-
B	Gauge boson	-	-	1
$L_\alpha = \begin{pmatrix} \nu_\alpha \\ e_\alpha \end{pmatrix}_L$	Left-handed leptons	1	2	-1/2
$(e_\alpha)_R$	Right-handed leptons	1	1	-1
$Q_\alpha = \begin{pmatrix} u_\alpha \\ d_\alpha \end{pmatrix}_L$	Left-handed quarks	3	2	1/6
$(u_\alpha)_R$	Right-handed up quarks	3	1	2/3
$(d_\alpha)_R$	Right-handed down quarks	3	1	-1/3
$\Phi = \begin{pmatrix} \phi^+ \\ \phi^0 \end{pmatrix}$	Complex scalar	1	2	1/2

Table 2.1: Standard Model particle content before electroweak symmetry breaking [13].

where $G^\alpha_{\mu\nu}$ is the gluon field strength tensor

$$G^\alpha_{\mu\nu} = \partial_\mu G^\alpha_\nu - \partial_\nu G^\alpha_\mu - g_s f^{\alpha\beta\gamma} G_{\mu\beta} G_{\nu\gamma}, \quad \alpha,\beta,\gamma = 1,2,...,8, \tag{2.3}$$

with g_s the strong coupling constant and $f_{\alpha\beta\gamma}$ are the $SU(3)$ group structure constants. $W^\alpha_{\mu\nu}$ is the $SU(2)_L$ gauge boson field strength tensor

$$W^\alpha_{\mu\nu} = \partial_\mu W^\alpha_\nu - \partial_\nu W^\alpha_\mu - g\varepsilon^{\alpha\beta\gamma} W_{\mu\beta} W_{\nu\gamma}, \quad \alpha,\beta,\gamma = 1,2,3, \tag{2.4}$$

where g is the weak coupling constant and $\varepsilon_{\alpha\beta\gamma}$ are the $SU(2)$ structure constants. $B_{\mu\nu}$ is the $U(1)_Y$ field strength tensor

$$B_{\mu\nu} = \partial_\mu B_\nu - \partial_\nu B_\mu. \tag{2.5}$$

The fermion kinetic terms have the form of the free Dirac kinetic term

$$\mathscr{L}_F = \overline{\psi} i\gamma^\mu \partial_\mu \psi, \tag{2.6}$$

with the substitution

$$\partial_\mu \to D_\mu, \tag{2.7}$$

where D_μ, is the covariant derivative. This substitution ensures gauge invariance, and the form of the covariant derivative for each fermion field

depends on its gauge transformation properties. For the quark doublets Q, the covariant derivative is

$$D_\mu = \partial_\mu I + \frac{ig}{2}\vec{\tau}\cdot\vec{W}_\mu + \frac{ig'}{6}IB_\mu + \frac{ig_s}{2}I\vec{\lambda}_{\alpha\alpha'}\cdot\vec{G}_\mu, \tag{2.8}$$

where g' is the $U(1)_Y$ coupling constant, τ are the 2-dimensional representations of $SU(2)$ and λ are the 3-dimensional representations of $SU(3)$. For right-handed quarks

$$D_\mu = \partial_\mu + ig'YB_\mu, \tag{2.9}$$

with $Y = 2/3$ for up-type quarks and $Y = -1/3$ for down quarks. For lepton doublets

$$D_\mu = \partial_\mu I + \frac{ig}{2}\vec{\tau}\cdot\vec{W}_\mu - \frac{ig'}{2}IB_\mu, \tag{2.10}$$

and for right-handed charged leptons

$$D_\mu = \partial_\mu - ig'B_\mu. \tag{2.11}$$

Note that mass terms are strictly forbidden in the gauge invariant Lagrangian for chiral fermions and gauge bosons. This contradicts the observation of nonzero masses for the physical Z and W bosons, and of the masses of leptons. The solution of this problem is the spontaneous breaking of the gauge group by the scalar field Φ. Given that Φ is a Lorentz scalar, it is the only particle in the SM which can develop a non-zero vacuum expectation value (vev) without breaking Lorentz invariance. Φ is uncharged under $SU(3)_C$, so this symmetry remains unbroken. Because the breaking of the electroweak sector is independent of the strong sector we can analyze it independently from it. This allows us to neglect strong interactions from this point forward. The breaking of $SU(2)_L \times U(1)_Y$ proceeds as follows:

1. The minimum of the scalar potential, dictated by the couplings of the scalar potential, lies outside $\Phi = 0$.

2. Φ is expanded around the minimum, the true vacuum, as $\Phi = \langle\Phi\rangle + \phi$, where ϕ is a physical field.

3. The gauge fields W^i and B acquire mass terms from the Higgs kinetic term, which mixes them to produce the mass eigenstates $W^\pm$, Z and A.

First we find the vacuum of the theory, by minimizing the scalar potential. The scalar doublet can be written, in $SU(2)_L$ space, as

$$\Phi = \begin{pmatrix} \phi_1 + i\phi_2 \\ \phi_3 + i\phi_4 \end{pmatrix}, \tag{2.12}$$

where each ϕ_i is a real scalar field. The vev of the fields may be aligned so that only $\langle \phi_3 \rangle = \mathrm{v} \neq 0$. With this vev alignment we obtain the tadpole equation for the vev

$$\frac{dV(\Phi)}{d\Phi}|_{\phi_i=0} = \mu^2 \mathrm{v} + \lambda \mathrm{v}^3 = 0, \tag{2.13}$$

so the minimum of the potential is

$$\mathrm{v} = \sqrt{\frac{-\mu^2}{\lambda}} \tag{2.14}$$

for $\mu^2 < 0$. Schematically the potential has the shape illustrated in Fig.(2.1) The breaking of a continuous symmetry should result in the appearance of massless scalar states according to the Goldstone theorem. The Higgs-Englert-Brout mechanism ensures that the Goldstone bosons produced from breaking gauge symmetries are not physical states, but are eaten by the gauge bosons of the broken gauge group. This is the mechanism by which gauge bosons become massive. This disappearance of physical degrees of freedom of the scalar sector is made explicit in the unitary gauge. After rewriting the scalar kinetic terms in the unitary gauge, where Φ is written as

$$\Phi = \begin{pmatrix} 0 \\ \mathrm{v} + H \end{pmatrix}, \tag{2.15}$$

the gauge bosons W and B acquire mass terms through the Higgs field kinetic term, the quarks and down-type leptons obtain mass terms through the Yukawa couplings, and the only physical degree of freedom of Φ that remains is a neutral scalar H. The charged bosons $W^{\pm}$ resulting from the mixing of W^1 with W^2 acquire the mass

$$M^2_{W^{\pm}} = \frac{1}{4} g^2 \mathrm{v}^2. \tag{2.16}$$

The W^3 and B bosons mix to form the mass eigenstates Z and A, in the following manner

$$\begin{bmatrix} Z_\mu \\ A_\mu \end{bmatrix} = \begin{bmatrix} \cos\theta_W & \sin\theta_W \\ -\sin\theta_W & \cos\theta_W \end{bmatrix} \begin{bmatrix} W^3_\mu \\ B_\mu \end{bmatrix}, \tag{2.17}$$

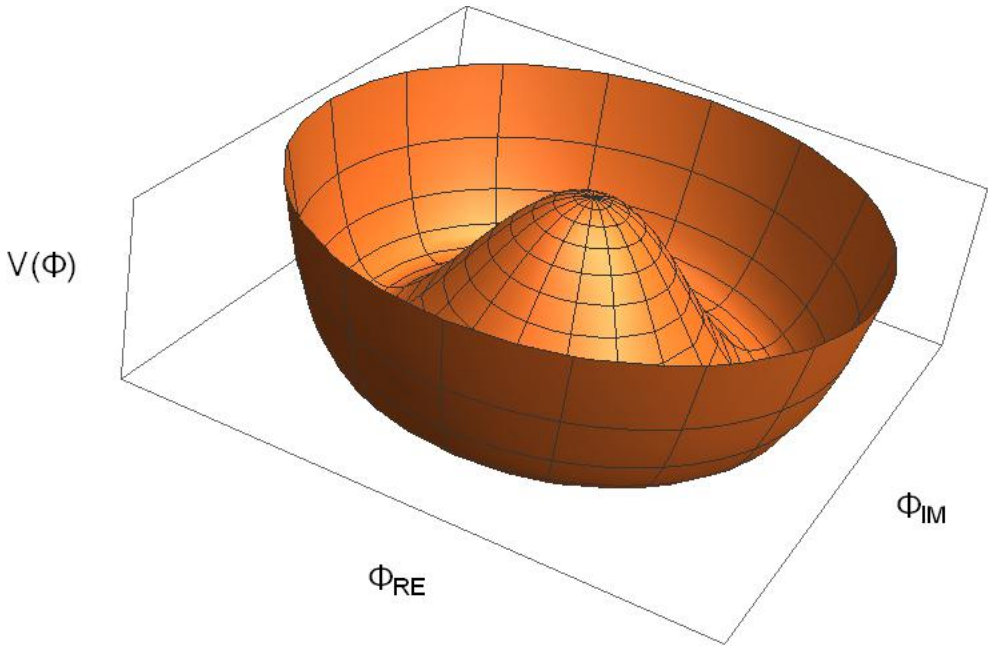

Figure 2.1: Schematic illustration of the Higgs potential. The minimum of the potential lies outside of zero, because of the choice of the values of the parameters of the potential. The breaking of $SU(2)_L \times U(1)_Y$ arises from the non-invariance of the base state of this potential under the group transformations.

where the mixing angle θ_W, the Weinberg angle, is defined as follows

$$\sin\theta_W = \frac{g'}{\sqrt{g^2+g'^2}}, \tag{2.18}$$

from which the cosine of the angle is

$$\cos\theta_W = \frac{g}{\sqrt{g^2+g'^2}}. \tag{2.19}$$

The A boson remains massless and the Z boson acquires the mass

$$M_Z^2 = \frac{1}{4}\mathrm{v}^2(g^2+g'^2). \tag{2.20}$$

From eqs.(2.16-2.20) we obtain a prediction for the masses M_W, M_Z and $\cos\theta_W$

$$M_W^2 = M_Z^2 cos^2\theta_W, \tag{2.21}$$

at tree level. This prediction is valid when W and Z bosons acquire masses from scalar doublets. This relationship is confirmed experimentally at an accuracy of 0.1% ([14]) , severely limiting the scalar sector of $SU(2)_L \times U(1)_Y$ and the mechanism of its breaking.
The breaking of $SU(2)_L \times U(1)_Y$ by the scalar vev leaves behind a remnant symmetry $U(1)_Q$, generated by the combination of the generators τ_3 and Y of the original gauge group. The massless boson A is identified as a photon, and its masslessness is guaranteed at all levels of perturbation theory by the remnant $U(1)_Q$.
In the fermion sector the Yukawa couplings generate masses after EW symmetry breaking. The relevant couplings in the lagrangians are

$$\mathscr{L}_f = -\sum_{\alpha,\beta=1}^{3}\left[\frac{vY^u_{\alpha\beta}}{\sqrt{2}}\overline{u_{\alpha L}}u_{\beta R} + \frac{vY^d_{\alpha\beta}}{\sqrt{2}}\overline{d_{\alpha L}}d_{\beta R} + \frac{vY^l_{\alpha\beta}}{\sqrt{2}}\overline{e_{\alpha L}}e_{\beta R} + h.c. \quad ,\right], \tag{2.22}$$

generating the Dirac mass matrices

$$\mathscr{M}^f = \frac{Y^f}{\sqrt{2}}v, \tag{2.23}$$

with $f = u,d,l$ designates up-quarks, down-quarks and charged leptons respectively. These matrices are not necessarily diagonal, a change of basis is required to arrive at the mass eigenstates of the theory. For each

fermion type the left-handed and right-handed parts are transformed independently through the $R^f_{L/R}$ matrices, such that the mass eigenstates are written as

$$f'_{\alpha L/R} = R^f_{\alpha\beta} f_{\beta L/R}. \tag{2.24}$$

Under this transformation the mass matrices transform as

$$R^{u\dagger}_L M^u R^u_R = \begin{pmatrix} m_u & 0 & 0 \\ 0 & m_c & 0 \\ 0 & 0 & m_t \end{pmatrix}, \tag{2.25}$$

$$R^{d\dagger}_L M^d R^d_R = \begin{pmatrix} m_d & 0 & 0 \\ 0 & m_s & 0 \\ 0 & 0 & m_b \end{pmatrix}, \tag{2.26}$$

$$R^{l\dagger}_L M^l R^l_R = \begin{pmatrix} m_e & 0 & 0 \\ 0 & m_\mu & 0 \\ 0 & 0 & m_\tau \end{pmatrix}. \tag{2.27}$$

In the Standard Model Lagrangian the interaction of fermions with the Z, the photon and the physical scalar H are unaffected by these transformations. In the charged current interaction, the operators with $W^\pm$ bosons, the transformation matrices for the left-handed up type quarks and down type quarks appear and have a physical effect in the quark sector. In the lepton sector the charged current interaction appears with the transformations for left-handed neutrinos and charged leptons. The combination appearing in these terms are

$$U_{CKM} = R^{u\dagger}_L R^d_R, \tag{2.28}$$

$$U_{PMNS} = R^{l\dagger}_L R^\nu_R, \tag{2.29}$$

the first one in quark interactions and the second one in lepton interactions. There are 3 generations of particles in the Standard Model, making these matrices 3-dimensional. In general they can be parametrized by three Euler angles and 3 complex phases, but due to the freedom to absorb nonphysical phases in Dirac fields it is possible to absorb two phases for quarks, and for leptons if neutrinos are not Majorana particles. The phases make the matrices complex, and thus introduce Charge-Parity (CP)

violation to the Standard Model. The mixing matrix of the quark sector is written in the PDG parametrization as follows

$$U_{CKM} = \begin{pmatrix} c_{12}c_{13} & s_{12}c_{13} & -s_{13}e^{-i\delta_{CKM}} \\ -s_{12}c_{23} - c_{12}s_{23}s_{13}e^{i\delta_{CKM}} & c_{12}c_{c23} - s_{12}s_{13}e^{i\delta_{CKM}} & s_{23}c_{13} \\ s_{12}s_{23} - c_{12}c_{23}s_{13}e^{i\delta_{CKM}} & -c_{12}s_{23} - s_{12}c_{23}s_{13}e^{i\delta_{CKM}} & c_{23}c_{13} \end{pmatrix} \quad (2.30)$$

In the quark sector CP violating phenomena have been observed, suggesting a value of the CKM complex phase around [14]

$$\delta_{CKM} \sim 1.2 \pm 0.08 rad. \quad (2.31)$$

CP violation in the Standard Model is a subject of great interest, due to its possible connection to Baryogenesis, the unknown mechanism which results in the matter-antimatter imbalance of the Universe. The observed value for δ_{CKM} is too small to account for the observed imbalance [15], but a large enough value of its equivalent in the lepton sector may explain this phenomenon [16].

Chapter 3

Massive Neutrinos in the Standard Model and Beyond

3.1 Majorana fermions

The Dirac field equation defines a spin 1/2 particle. The field equation is

$$(i\gamma^\mu \partial_\mu - m)\Psi = 0, \tag{3.1}$$

which can be derived from the field Lagrangian density

$$\mathscr{L}_D = \bar{\Psi}(i\gamma^\mu \partial_\mu - m)\Psi, \tag{3.2}$$

where $\bar{\Psi} = \psi\dagger\gamma^0$. The gamma matrices γ^μ are a set of 4 matrices of dimension 4 defined by the conditions

$$\{\gamma^\mu, \gamma^\nu\} = 2g^{\mu\nu}, \tag{3.3}$$

$$\gamma_0\gamma_\mu\gamma_0 = \gamma_\mu\,\dagger\,. \tag{3.4}$$

The general solution for the Dirac equation is a Dirac fermion, which can be written as a Fourier expansion in the following manner

$$\Psi(x) = \sum_s \int_p \left(a_s(p)\tilde{u}_s(p)e^{-ip\cdot x} + b_s^\dagger(p)\tilde{v}_s(p)e^{ip\cdot x}\right), \tag{3.5}$$

where u, v are the Dirac spinors, the plane wave solutions. This solutions have 4 degrees of freedom, physically corresponding to the two possible chiralities for the particle and antiparticle.
The set of matrices obeying (3.4) is not unique, a similarity transformation

defined by a unitary matrix U can generate another basis $\tilde{\gamma^\mu}$ from a given basis γ^μ

$$\tilde{\gamma^\mu} = U\gamma^\mu U^\dagger. \tag{3.6}$$

The question arises then, can the Dirac equation be purely real, and therefore have real solutions? Evidently if all the entries of the γ^μ matrices can be made purely imaginary, or zero, the Dirac equation would then be real. As first found by Majorana [17] we can write down a set of matrices obeying (3.4) with only imaginary entries and zeroes, as shown below

$$\begin{aligned} \tilde{\gamma^0} = \begin{pmatrix} 0 & \sigma^2 \\ \sigma^2 & 0 \end{pmatrix}, \tilde{\gamma^1} = \begin{pmatrix} i\sigma^1 & 0 \\ 0 & i\sigma^1 \end{pmatrix}, \\ \tilde{\gamma^2} = \begin{pmatrix} 0 & \sigma^2 \\ -\sigma^2 & 0 \end{pmatrix}, \tilde{\gamma^0} = \begin{pmatrix} i\sigma_3 & 0 \\ 0 & i\sigma_3 \end{pmatrix}, \end{aligned} \tag{3.7}$$

where σ^i are the usual Pauli matrices. This is the Majorana basis for the γ^μ matrices, where

$$\tilde{\gamma^\mu}^* = -\tilde{\gamma^\mu}, \tag{3.8}$$

adopting the convention of using a tilde accent to denote the gamma matrices in this basis, and the solutions for the Dirac equation in this basis. Now that we have imposed a reality condition on the Dirac equation through the use of the Majorana basis we can search for real solutions to the equation of motion. This solutions will obey

$$\tilde{\Psi}^* = \tilde{\Psi}, \tag{3.9}$$

and we will call them Majorana fermions. Note that the reality condition (3.9) for the solutions of the Dirac equation holds only in the Majorana basis, a change of γ^μ basis comes with a change of basis in the solutions Ψ, to maintain the invariance of the Lagrangian under such transformations. The basis change defined by the unitary matrix U is given by

$$\begin{aligned} \tilde{\gamma^\mu} &= U\gamma^\mu U^\dagger, \\ \tilde{\Psi} &= U\Psi. \end{aligned} \tag{3.10}$$

With this transformation rules in mind we can write down the Majorana condition (3.9) in an arbitrary basis as follows. Transforming the condition with U we immediately obtain

$$U^\dagger\Psi = (U^\dagger\Psi)^*, \tag{3.11}$$

from which we can write, using the unitarity of U,

$$\Psi = UU^T\Psi^*. \tag{3.12}$$

The unitarity of U guarantees the unitarity of UU^T. It is standard to define the Majorana condition with a matrix C, obtained from

$$\gamma_0 C = UU^T. \tag{3.13}$$

With this definition we write the Majorana condition in its common form

$$\Psi = \gamma_0 C\Psi^*, \tag{3.14}$$

which is valid in any basis. Returning to the Majorana basis, we can write down the Fourier expansion of a solution to the Dirac equation

$$\tilde{\Psi}(x) = \sum_s \int_p \left(a_s(p)\tilde{u}_s(p)e^{-ip\cdot x} + a_s^\dagger(p)\tilde{u}_s^*(p)e^{ip\cdot x} \right), \tag{3.15}$$

where the sum over s is over spin states. This solution is given in terms of the spinors $\tilde{u}$ in the Majorana basis. Note that the two terms of the solution are complex conjugate of each other, guaranteeing that $\tilde{\Psi}$ is real.
Now, if we use the chiral basis for spinors, where the γ^μ matrices take a block diagonal form, a 4-spinor can be written in terms of 2-spinors as follows

$$\Psi = \begin{pmatrix} \xi_1 \\ \xi_2 \end{pmatrix}, \tag{3.16}$$

and using the Majorana condition in this basis

$$(\gamma_0 C)_{chiral} = \begin{pmatrix} 0 & i\sigma^2 \\ -i\sigma^2 & 0 \end{pmatrix} \tag{3.17}$$

$$\therefore \xi_2 = -i\sigma_2\xi_1^* \quad , \quad \xi_1 = i\sigma_2\xi_2^*. \tag{3.18}$$

This equation relates one 2-spinor with another, eliminating degrees of freedom of the field. We can therefore write the Majorana field in this basis as

$$\Psi = \begin{pmatrix} \xi \\ -i\sigma_2\xi^* \end{pmatrix}. \tag{3.19}$$

With this in mind the Dirac Lagrangian for the Majorana field becomes

$$\mathscr{L} = \frac{i}{2}(\xi^\dagger\sigma^\mu\partial_\mu\xi - m\xi^T\sigma^2\xi) = \frac{1}{2}(\xi^\dagger i\sigma^\mu\partial_\mu\xi - m\xi\bar{C}\xi), \tag{3.20}$$

where we have identified the first field in the mass term as the charge conjugated field. The mass term in this Lagrangian is the Majorana mass term. Contrast this term with the Dirac mass term that Standard Model fermions have

$$\mathscr{L}_{Dirac} = -m\bar{\xi}_1\xi_2, \tag{3.21}$$

which is formed from the two independent chiral bispinors. From the first form of the Majorana mass term it is obvious that any $U(1)$ charge carried by the Majorana field is broken by the mass term, since under a $U(1)$ transformation the Majorana field and mass terms transform as

$$\xi \to e^{i\theta}\xi \quad \therefore \quad -m\xi^T\sigma^2\xi \to -me^{i2\theta}\xi^T\sigma^2\xi, \tag{3.22}$$

making this term not invariant under $U(1)$. This applies both to global and gauge symmetries, which is why neutrinos are the only Standard Model particles that may be Majorana, since they are the only electrically neutral fermions. A charged particle with Majorana mass would spoil $U(1)_Q$, which we know is a good symmetry. A global $U(1)$ which could be broken by Majorana neutrinos, and which we don't know if it is a good symmetry is lepton number L. Lepton number is an accidental symmetry of the Standard Model, under which charged leptons and neutrinos have charge $L = +1$ and charged antileptons and antineutrinos are charged $L = -1$. The Lagrangian of the Standard Model preserves this symmetry, which guarantees the accidental conservation of L perturbatively. If neutrinos are Majorana particles then L is not conserved, and the Majorana mass term predicts perturbative processes where $|\Delta L| = 2$.

3.2 Massive neutrinos

As shown in the last section, the matter content of the Standard Model does not allow for massive neutrinos. The observation of neutrino oscillations indicate that there are at least two neutrino mass eigenstates with nonzero mass.

In general the mass terms are not diagonal in the interaction basis, so it is necessary to rotate the lepton states from the interaction basis, defined by the gauge invariant Lagrangian, to the mass eigenstate basis using the complex rotation matrices V_ν for neutrinos and V_l for charged leptons. This rotation affects only charged current interactions in the SM, where the combination

$$U_{MNSP} = V_l^\dagger V_\nu, \tag{3.23}$$

appears. In the three neutrino case this matrix is defined by three euler angles θ_{ij} and one CP violating phase δ_{CP}. If neutrinos are Majorana particles an additional matrix, containing two phases, is necessary to relate the two basis. This phases, however, can be absorbed either by the rotation matrix U_{MNSP} or by the masses themselves. Here we absorb the phases in the neutrino masses, making the diagonal neutrino mass matrix complex. Additionally the physical phases are the phase differences between neutrinos, so we choose to insert the phases in the second and third neutrino mass eigenstates. The transformation from the interaction basis to the basis where charged leptons are diagonal is given by

$$\nu_\alpha^f = (U_{MNSP})_{\alpha\beta}\nu_\beta^m, \tag{3.24}$$

where ν^f are the interaction eigenstates, and ν^m the mass eigenstates. The PDG convention writes the matrix in the following form

$$U_{MNSP} = \begin{pmatrix} c_{12}c_{13} & s_{12}c_{13} & -s_{13}e^{-i\delta} \\ -s_{12}c_{23} - c_{12}s_{23}s_{13}e^{i\delta} & c_{12}c_{c23} - s_{12}s_{13}e^{i\delta} & s_{23}c_{13} \\ s_{12}s_{23} - c_{12}c_{23}s_{13}e^{i\delta} & -c_{12}s_{23} - s_{12}c_{23}s_{13}e^{i\delta} & c_{23}c_{13} \end{pmatrix} \tag{3.25}$$

with the shorthand notation $c_{ij} = cos\theta_{ij}$ and $s_{ij} = sin\theta_{ij}$. Under this rotation the mass matrix transforms from the interaction basis to the mass basis in the following manner

$$(M_\nu^I)^2 = U_{MNSP}^T (M^m)^2 U_{MNSP}, \tag{3.26}$$

where $M^m = diag(\mu_1, \mu_2, \mu_3)$, in our convention μ_1 is a real positive number. Note that another common convention makes μ_3 the real mass, and these two convention are related by a global phase shift, leading to the same physical observables.
The neutrino oscillation probability can be written using this matrix and masses as

$$P_{\alpha\beta}(E,L) = |\sum_i U_{\alpha i}^* U_{\beta i} e^{i\frac{m_i^2 L}{2E}}|^2 \tag{3.27}$$

$$= \delta_{\alpha\beta} - 4\sum_{i>j} Re(U_{\alpha i}^* U_{\beta i} U_{\alpha j} U_{\beta j}^*) sin^2\left(\frac{\Delta m_{ij}^2 L}{4E}\right) \tag{3.28}$$

$$+2\sum_{i>j} Im(U_{\alpha i}^* U_{\beta i} U_{\alpha j} U_{\beta j}^*) sin\left(\frac{\Delta m_{ij}^2 L}{2E}\right), \tag{3.29}$$

where $P_{\alpha\beta}(E,L)$ is the probability of detecting a neutrino emitted in the flavor α with an energy E at a distance L as a neutrino of flavor β. From the

Parameter	Best-fit	3σ range
δm^2_{21} [10^{-5} eV^2]	7.37	6.93 - 7.97
$\lvert\delta m^2\rvert$ [10^{-3} eV^2]	2.50 (2.46)	2.37 - 2.63 (2.33 - 2.60)
$sin^2\theta_{12}$	0.297	0.250 - 0.354
$sin^2\theta_{23}$, $\delta m^2 > 0$	0.437	0.379 - 0.616
$sin^2\theta_{23}$, $\delta m^2 < 0$	0.569	0.383 - 0.637
$sin^2\theta_{13}$, $\delta m^2 > 0$	0.0214	0.0185 - 0.0246
$sin^2\theta_{13}$ $\delta m^2 < 0$	0.0218	0.0186 - 0.0248
δ/π	1.35 (1.32)	0.92 - 1.99(0.83 - 1.99)

Table 3.1: Mixing parameters obtained from fits of oscillation experiment results [18].

last expression given for the probability it is obvious that oscillation experiments can measure angles and squared mass differences, but not Majorana phases or the absolute mass scale of neutrinos. It can, however, measure the CP violating angle δ, which may be related to the matter-antimatter imbalance of the Universe [16]. In Fig. (3.1) we show one of the current fits for the oscillation parameters from various experiments [18].

Oscillation experiments are sensitive to squared mass differences, but not to the absolute scale of the neutrino masses. The most sensitive direct searches for neutrino masses are the measurements of the electron energy spectrum of beta decay. The observed process is

$$(A,Z) \rightarrow (A,Z+1) + e^- + \bar{\nu}, \tag{3.30}$$

where (A,Z) is a nucleus with A nucleons and Z protons. Neutrino masses affect the kinematics of the process, which can be, in principle, observed in a distortion of the shape of the energy spectrum of the emitted electron. This experiment can measure the effective electron mass m_{ν_e}

$$m^2_{\nu_e} = \sum_i |U_{ei}|^2 m_i^2. \tag{3.31}$$

The current experimental bounds on m_{ν_e} come from the tritium beta decay experiments Troitsk [19] and Mainz [20]

$$\begin{aligned} m^{\text{Troitsk}}_{\nu_e} &< 2.05\ eV \\ m^{\text{Mainz}}_{\nu_e} &< 2.3\ eV. \end{aligned} \tag{3.32}$$

From cosmological observations, in conjunction with a cosmological model, one can derive a limit on the sum of neutrinos masses [21]

$$\sum_i m_{\nu_i} < 0.12eV, \tag{3.33}$$

which is stronger than direct limits, but depends on cosmological model parameters.
The smallness of this bounds is at odds with the mass generation mechanism of the Standard Model, which produces masses from a $10^2 GeV$ higgs vev.

3.2.1 Neutrino masses in $SU(2)_L \times U(1)_Y$ gauge theory

The Standard Model does not contain right-handed neutrinos, unlike every other fermion in the theory. The Standard Model is built this way precisely to prohibit the generation of neutrino masses at all orders in perturbation theory. Completing the Standard Model with 3 generations of right-handed neutrinos N_α, transforming under $G_{SM} = SU(3)_C \times SU(2)_L \times U(1)_Y$ as

$$N_R \sim (1,1,1), \tag{3.34}$$

we obtain a Yukawa coupling for neutrinos

$$\mathscr{L}_\nu = Y^\nu_{\alpha\beta} \bar{L}_\alpha \tilde{\Phi} N, \tag{3.35}$$

which after EW symmetry breaking generates the Dirac mass terms

$$\mathscr{L}_D = Y^\nu_{\alpha\beta} \mathrm{v} \bar{\nu}_\alpha N. \tag{3.36}$$

Additionally, the right-handed neutrinos can form the Majorana mass terms

$$\mathscr{L}_N = M_{\alpha\beta} \bar{N^c} N. \tag{3.37}$$

The scale of the Majorana mass terms is arbitrary, in principle, or it could be generated by the breaking of higher-scale symmetries. In the case where $M >> vY^\nu$, the mixing of N with ν produces 6 Majorana neutrino eigenstates, 3 light neutrinos, which are mostly active neutrinos, and 3 heavy neutrinos, which are mostly sterile. This mechanism for light neutrino mass generation is called the type I seesaw mechanism [22]. It is a UV completion of the Weinberg dimension-5 operator [23]

$$\mathscr{L}_W = \frac{g_W}{\Lambda} \bar{L^c} \Phi \Phi L, \tag{3.38}$$

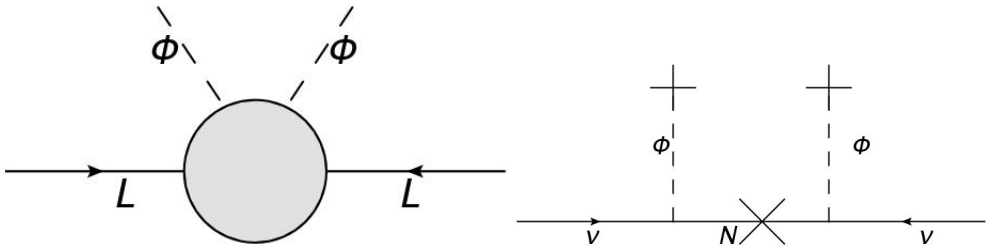

Figure 3.1: Left. Effective dimension-5 Weinberg operator [23] leading to light neutrino Majorana masses. This is the lowest dimension, electroweak invariant operator which can account for neutrino masses in the Standard Model. This operator violates lepton number by two units. The high-energy mechanism giving rise to the operator, the UV completion, is contained within the gray blob of the diagram. Right. Type-I seesaw mechanism [22, 24–27] for neutrino Majorana masses. The completion of the Weinberg operator is achieved by introducing a G_{SM} singlet fermion N for each family of neutrinos. It naturally results in sub-eV neutrino masses for N masses larger than $\sim 10^{13}$ GeV, for unit order Yukawa couplings.

which is $SU(2)_L \times U(1)_Y$ invariant, and generates Majorana neutrino masses after EW symmetry breaking. The resulting mass matrix in the $(\nu_\alpha N_\alpha)$ basis is given by the block matrix

$$M_{TypeI} = \begin{pmatrix} 0 & m_D \\ m_D^T & M \end{pmatrix}. \tag{3.39}$$

In the $M >> vY^\nu$ limit the light neutrino mass matrix m_l and the heavy neutrino matrix m_h generated by this mechanism are given by

$$m_l \approxeq -m_D^T M^{-1} m_D, \tag{3.40}$$

$$m_h \approxeq M, \tag{3.41}$$

at first order in m_D/M, where m_D is the Dirac mass matrix. To generate the sub-eV light neutrino masses required by tritium decay experiments when the Dirac term Yukawa couplings are of order $\mathcal{O}(1)$ the sterile neutrinos masses must be heavier than 10^{13} GeV , which is close to the GUT scale $\sim 10^{15} GeV$. Another two seesaw mechanisms for Majorana masses are illustrated in Fig. (3.2). These three seesaw mechanisms complete the $\mathscr{L}_W$ operator at tree level, using $SU(2)_L$ triplets or singlets. In these completions of the Weinberg operator the smallness of neutrino masses is explained by the heaviness of the intermediate particles. The Weinberg operator can also be completed at loop order, the smallness of neutrino masses can be

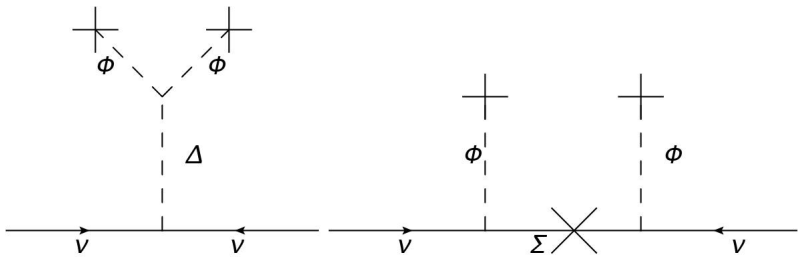

Figure 3.2: Left. Type-II seesaw mechanism for neutrino masses [27]. The UV completion of the Weinberg operator is obtained by adding a scalar transforming as $(1,3,0)$ under the Standard Model gauge group.Right. Type-III seesaw mechanism for neutrino masses [28]. The UV completion of the Weinberg operator is obtained by adding a fermion transforming as $(1,3,0)$ under the Standard Model gauge group.

explained in these frameworks from the loop factors $(4\pi)^{-2N}$ arising from N-loops, and from the heavy particles appearing inside the loop.

3.2.2 Neutrinoless double beta decay

A promising phenomenon to determine the Majorana nature of neutrinos is neutrinoless double beta decay ($0\nu\beta\beta$), the simultaneous beta decay of two neutrons within a nucleus yielding no outgoing neutrinos

$$2n \to 2p + 2e^-, \tag{3.42}$$

or in terms of nuclear processes

$$(A,Z) \to (A,Z+2) + 2e^- + Q_{\beta\beta}, \tag{3.43}$$

where $Q_{\beta\beta}$ is the energy released in the process. This process violates lepton number by two units ($\Delta L = 2$), if neutrinos are Majorana particles $0\nu\beta\beta$ could be an observable process. Although Majorana neutrinos are not the only BSM physics contributing to $0\nu\beta\beta$ [29], this process can be used to constrain the values of neutrino masses. Additionally, the Schechter-Valle theorem guarantees Majorana masses for neutrinos in the presence of any mechanism giving rise to $0\nu\beta\beta$ [30], as can be seen from Fig (3.3). Given the theoretical interest of this phenomenon, several experiments have been carried out in search of it. The search of it has proven to be challenging, in both the experimental and the theoretical fronts. The current limits on the half-life of this process have reached the range [32]

$$T_{1/2}^{0\nu\beta\beta} > 10^{25} - 10^{26}\text{years}, \tag{3.44}$$

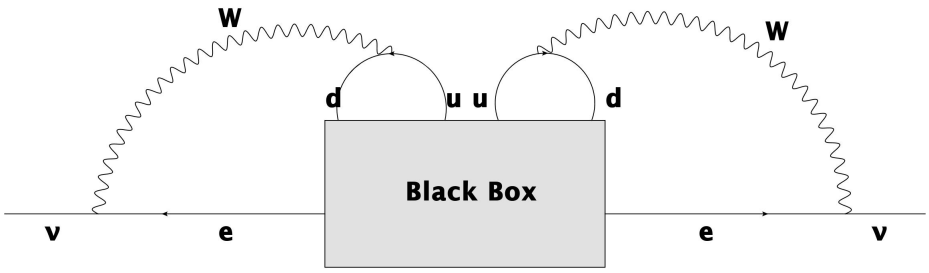

Figure 3.3: Black Box theorem [30]. This Standard Model diagram guarantees nonzero Majorana masses for neutrinos in the presence of any mechanism giving rise to $0\nu\beta\beta$ inside the black box. An analysis of the effect of the operators leading to $0\nu\beta\beta$ on the lifetime $T^{0\nu}_{1/2}$ and on the induced Majorana masses shows that the current limits on the decay lifetime impose bounds on the operators leading to Majorana masses far too strict to account for the observed neutrino oscillation parameters Δm^2_{12} and Δm^2_{13} [31]. This excludes this types of operators as leading contributors to neutrino masses.

with forthcoming experiments promising to increase their sensitivity up to two orders of magnitude.
In the Standard Model extended with neutrino Majorana masses the diagram resulting in $0\nu\beta\beta$ is given by Fig. (??). The half-life for this process, assuming this diagram is the only contributor, can be written as

$$(T_{1/2}^{0\nu\beta\beta})^{-1} = G^{0\nu} \times |M^{0\nu}|^2 \times \langle m_{\beta\beta} \rangle^2, \tag{3.45}$$

where $G^{0\nu}$ is the phase space factor, $M^{0\nu}$ is the nuclear transition matrix element, and $m_{\beta\beta}$ is the effective Majorana mass

$$\langle m_{\beta\beta} \rangle^2 = |\sum_i U_{ei}^2 m_(\nu_i)|^2. \tag{3.46}$$

The neutrino mixing matrix U contains both the Dirac and Majorana phases δ and α_i. Assuming there are only three active neutrinos, which means there is only one Dirac phase and two Majorana phases, and using the PDG parametrization of U we can write the effective Majorana mass as follows

$$\langle m_{\beta\beta} \rangle = |c_{12}^2 c_{13}^2 m_1 + s_{12}^2 c_{13}^2 m_2 e^{i\alpha_2} + s_{13}^2 m_3 e^{i(\alpha_3 - 2\delta)}|, \tag{3.47}$$

where we have adopted the notation $s_{ij} = sin\theta_{ij}$ and $c_{ij} = cos\theta_{ij}$. The presence of Majorana and Dirac phases in the sum allows for relative minus signs between the terms in the sum, opening up the possibility of cancellations.
The nuclear transition matrix element is the biggest source of theoretical uncertainty. To calculate $|M^{0\nu}|$ one needs to evaluate nuclear structure transitions from the initial nucleus to the final state, as well as properly expressing the nuclear-lepton interaction lagrangian in terms of the quark-lepton interaction lagrangian. Both of these steps are highly non-trivial, and the results from different approaches agree within one order of magnitude, which is the main source of the one order of magnitude uncertainty in $m_\beta\beta$ [33].
The most stringent measurement of the half-life of a neutrinoless double beta decay mode is by the KamLAND-Zen experiment [32]. This experiment used ^{136}Xe as a parent nucleus, yielding a lower limit on the lifetime of the decay of

$$T_{\beta\beta}^{0\nu} > 1.07 \times 10^{26} \text{ years} \tag{3.48}$$

at 90% C.L. This translates to a limit on the effective Majorana mass of

$$\langle m_{\beta\beta} \rangle < (61 - 165) \text{ meV}, \tag{3.49}$$

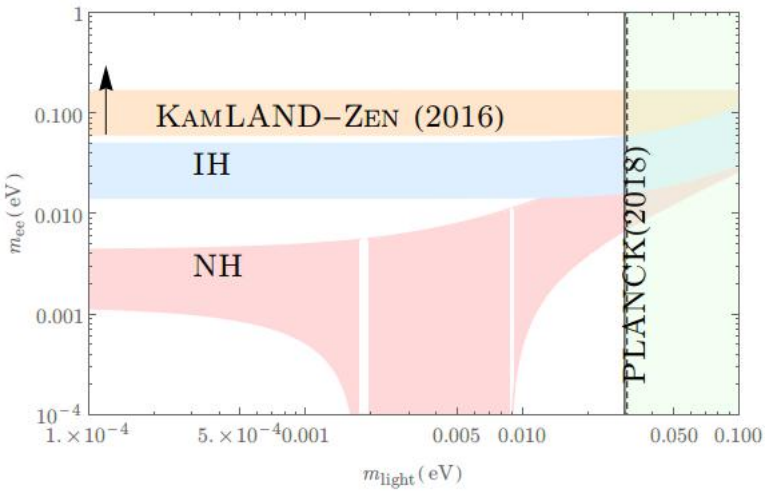

Figure 3.4: Allowed values of $m_{\beta\beta}$ from measurements of $T^{0\nu}_{1/2}$ of ^{136}Xe [32], cosmology [21], and neutrino oscillation parameters [18]. The KamLAND-Zen and Planck regions are exclusion limits, while the regions from oscillation data are allowed regions.

depending on the nuclear model used to calculate the nuclear transition matrix element. Combining the constraints from this experiment, the constraints from cosmology on neutrino masses from Planck [21], and the constraints from neutrino oscillation parameters we can obtain a plot of the allowed parameter space in the $\langle m_{\beta\beta}\rangle - m_{light}$ plane, as shown in Fig. (3.4). The constraints from neutrino oscillation parameters are obtained from varying the oscillation angles, within 3σ in eq. (3.47), and varying the complex phases in all angles. Note that for normal hierarchy ($m_1 < m_3$) a cancellation between terms of eq. (3.47) can lead to sub-10^{-4} eV effective neutrino masses, which are below the projected sensitivity of near-future experiments [34]. In the inverted hierarchy case there are no cancellations, and as such, it can be excluded in the case of non-observation of $0\nu\beta\beta$ in experiments with a sensitivity larger than $T^{0\nu}_{1/2} \sim 10^{28} y$, for most nuclei, and considering the worst case scenario for the values of the nuclear transition matrix elements [35].

Chapter 4

Lepton Flavor models

4.1 Fermion masses and discrete symmetries

The masses of fermions of the SM are determined by the Yukawa coupling with the Higgs field Φ

$$m_{ij}^{f} = Y_{ij}^{f} \langle \Phi \rangle \bar{f}_i f_j \tag{4.1}$$

where f is a family of fermions (u quarks ,d quarks or charged leptons). The observed values of SM fermion masses is given in Table (4.1). The masses of each fermion type spans several orders of magnitude, for example, up-type quark masses span from $\mathcal{O}(10^{-3}\text{GeV})$ to $\mathcal{O}(10^{2}\text{GeV})$. Given the singular value of the Higgs vev, $\langle \Phi \rangle = 246 GeV$, the following question arises: why are the masses of each generation of particles so far from each other?. Mathematically this is equivalent to asking: why are the eigenvalues of each matrix Y^f so different? Additionally the mismatch between the interaction basis states and the mass basis states, encoded in the mixing angles of the lepton and quark mixing matrices, introduces new unexplained parameters to the SM. An interesting way of naturally relating the observed mass spectrum in both the quark and lepton sectors to their mixing patterns is with the introduction of discrete symmetries to the Standard Model. Discrete flavor symmetries are defined by a discrete group G_F, under which Standard Model fields transform under matrix representations across generations, e.g.,

$$L_\alpha \to R_{\alpha\beta} L_\beta, \tag{4.2}$$

where $R_{\alpha\beta}$ is a matrix representation of an element of G_f. A Lagrangian invariant under this symmetry is formulated and additional fields are added to the SM, including scalar fields which acquire vevs necessary to break G_f

Field	Mass (GeV)
u	$2.2^{+0.5}_{-0.4} \times 10^{-3}$
s	$95^{+9}_{-3} \times 10^{-3}$
t	173 ± 0.4
d	$4.7^{+0.5}_{-0.3} \times 10^{-3}$
c	$1.275^{+0.025}_{-0.035}$
b	$4.18^{+0.04}_{-0.03}$
e	$(0.5109989461 \pm 0.0000000031) \times 10^{-3}$
μ	$0.1134289257 \pm 0.0000000025$
τ	1.77686 ± 0.00012

Table 4.1: Standard model fermion mass spectrum. Values from [14].

in order to produce phenomenologically viable masses and mixing angles. One of the attractive features of discrete groups in model building is the avoidance of additional gauge or goldstone bosons. Many discrete groups are regularly used in model building, including, but not limited to, S_3 [36], D_4, A_4 or $\Delta(27)$. In this work we will use the A_4 symmetry group, motivated by its status as the smallest group with an irreducible three dimensional representation. In the next section we proceed to describe the group.

4.2 A_4 group

A_4 is the group of even permutations of 4 objects, or the invariance group of a tetrahedron. We can denote an element of the group, a particular permutation $1234 \to n_1 n_2 n_3 n_4$, with the shorthand $(n_1 n_2 n_3 n_4)$. All elements of the group can be generated by the permutation S and T defined by

$$S = (4321) \quad , \quad T = (2314). \tag{4.3}$$

A_4 can be presented then with the equality

$$S^2 = T^3 = (ST)^3 = I. \tag{4.4}$$

Two elements of a group h_1 and h_2 are said to belong to the same equivalence class if there exists an element g of the group such that

$$g^{-1} h_1 g = h_2. \tag{4.5}$$

A_4 contains 4 equivalence classes, which are composed of the following elements

$$\begin{aligned} C_1 &: \quad I && (4.6)\\ C_2 &: \quad T,\quad ST,\quad TS,\quad STS && (4.7)\\ C_3 &: \quad T^2,\quad ST^2,\quad TS^2,\quad TST && (4.8)\\ C_4 &: \quad S,\quad T^2ST,\quad TST^2. && (4.9) \end{aligned}$$

In a finite group the sum of the square of the dimensions of irreducible representations of the group adds to the number of elements of the group. From this and from the property of the characters of elements on the representations A and B

$$\sum_{g\in G} \chi_g^A (\chi_g^B)^* = N\delta_A^B, \tag{4.10}$$

we can deduce that A_4 has 4 irreducible representations, three of dimension one (1,1',1") and one of dimension three (3).
For these representations we can write the generators of the group S and T, in the S diagonal basis, as follows

$$\begin{aligned} \mathbf{1}&: && S=1 \quad T=1\\ \mathbf{1}'&: && S=1 \quad T=\omega\\ \mathbf{1}''&: && S=1 \quad T=\omega^2\\ \mathbf{3}&: && S=\begin{pmatrix}1&0&0\\0&-1&0\\0&0&-1\end{pmatrix} \quad T=\begin{pmatrix}0&1&0\\0&0&1\\1&0&0\end{pmatrix}, \end{aligned} \tag{4.11}$$

where $\omega = e^{2i\pi/3}$. There is also an equivalent basis where T is diagonal instead of S, but we will work on this S diagonal basis.
The multiplication rules for the irreducible representations of A_4 are

$$\begin{aligned} \mathbf{3}\otimes\mathbf{3} &= \mathbf{1}\oplus\mathbf{1}'\oplus\mathbf{1}\oplus\mathbf{3_1}\oplus\mathbf{3}_2\\ \mathbf{1}\otimes\mathbf{1} &= \mathbf{1}\\ \mathbf{1}\otimes\mathbf{1}' &= \mathbf{1}'\\ \mathbf{1}\otimes\mathbf{1}'' &= \mathbf{1}''\\ \mathbf{1}\otimes\mathbf{3} &= \mathbf{3}\\ \mathbf{1}'\otimes\mathbf{1}' &= \mathbf{1}''\\ \mathbf{1}''\otimes\mathbf{1}'' &= \mathbf{1}'\\ \mathbf{1}'\otimes\mathbf{1}'' &= \mathbf{1}. \end{aligned} \tag{4.12}$$

	L_e	L_μ	L_τ	l_e	l_μ	l_τ	N_T	N_4	N_5	H	η	ϕ
$SU(2)_L$	2	2	2	1	1	1	1	1	1	2	2	1
A_4	α	β	γ	α	β	γ	3	δ	ε	1	3	3

Table 4.2: Matter content of the model. α, β, γ and ε denote any of the one-dimensional representations

The product of two triplets $a = (a_1, a_2, a_3)$ and $b = (b_1, b_2, b_3)$ in the S diagonal basis can be decomposed as follows

$$\begin{aligned}
\mathbf{1}: &\quad a_1b_1 + a_2b_2 + a_3b_3 \\
\mathbf{1}': &\quad a_1b_1 + a_2b_2\omega + a_3b_3\omega^2 \\
\mathbf{1}'': &\quad a_1b_1 + a_2b_2\omega^2 + a_3b_3\omega \\
\mathbf{3}_1: &\quad (a_2b_3, a_3b_1, a_1b_2) \\
\mathbf{3}_2: &\quad (a_3b_2, a_1b_3, a_2b_1).
\end{aligned} \tag{4.13}$$

From eq. (4.4) we see that S by itself generates Z_2 and T generates Z_3. This implies that the vev of a scalar ϕ triplet under A_4 which is invariant under S will preserve the Z_2 subgroup, while invariance under T preserves Z_3. The vev alignments which preserve these subgroups are as follows

$$\langle \phi \rangle = (v, v, v)_{Z_3}, \tag{4.14}$$
$$\langle \phi \rangle = (v, 0, 0)_{Z_2}. \tag{4.15}$$

4.3 Models for Dark Matter and neutrino masses with A_4

4.3.1 Model building

To obtain models for neutrino masses and mixings using the A_4 group we proceed as described before. First we add to the SM right-handed Neutrinos N to obtain Majorana masses from the seesaw mechanism. Next we assign representations of A_4 to the matter content of the lepton sector. Finally we add scalars transforming nontrivially under A_4 to break the discrete group and obtain phenomenologically viable masses and mixings. We propose then the matter content of table (4.2).

The five additional right-handed neutrinos are the triplet N_T and the singlets N_4 and N_5. The scalars η and ϕ will develop an A_4 breaking vev,

whose form will determine the residual symmetry. For an arbitrary assignment of α, β, γ and η representations the model lagrangian reads

$$\begin{aligned}
\mathscr{L}_Y &= y_e \overline{L}_e l_e H + y_\mu \overline{L}_\mu l_\mu H + y_\mu \overline{L}_\mu l_\mu H \\
&+ y_1^\nu \overline{L}_e \left[N_T \eta\right]_\alpha + y_2^\nu \overline{L}_\mu \left[N_T \eta\right]_\beta + y_3^\nu \overline{L}_\tau \left[N_T \eta\right]_\gamma \\
&+ y_4^{\nu 1} \delta_{\alpha\delta} \overline{L}_e N_4 H + y_4^{\nu 2} \delta_{\beta\delta} \overline{L}_\mu N_4 H + y_4^{\nu 3} \delta_{\gamma\delta} \overline{L}_\tau N_4 H \\
&+ y_5^{\nu 1} \delta_{\alpha\varepsilon} \overline{L}_e N_5 H + y_5^{\nu 2} \delta_{\beta\varepsilon} \overline{L}_\mu N_5 H + y_5^{\nu 3} \delta_{\gamma\varepsilon} \overline{L}_\tau N_5 H \\
&+ M \overline{N_T^c} N_T + M_4 \delta_{\delta 1} \overline{N_4^c} N_4 + M_5 \delta_{\varepsilon 1} \overline{N_5^c} N_5 \\
&+ y_2^{N_1} \delta_{1\delta} \left[\overline{N_T^c} \phi\right]_1 N_4 + y_2^{N_{1''}} \delta_{1''\delta} \left[\overline{N_T^c} \phi\right]_{1'} N_4 \\
&+ y_2^{N_{1'}} \delta_{1'\delta} \left[\overline{N_T^c} \phi\right]_{1''} N_4 + y_3^{N_1} \delta_{1\varepsilon} \left[\overline{N_T^c} \phi\right]_1 N_5 \\
&+ y_3^{N_{1''}} \delta_{1''\varepsilon} \left[\overline{N_T^c} \phi\right]_{1'} N_5 + y_3^{N_{1''}} \delta_{1'\varepsilon} \left[\overline{N_T^c} \phi\right]_{1''} N_5 \\
&+ y_1^N \left[\overline{N_T^c} \phi\right]_{3_1} N_T + (y_1^N)' \left[\overline{N_T^c} \phi\right]_{3_2} N_T \\
&+ M_{45} \delta_{\delta\varepsilon^*} \overline{N_4^c} N_5 + h.c
\end{aligned} \tag{4.16}$$

Notice that $\mathbf{1}'^* = \mathbf{1}''$ implies $\mathbf{1}' \times \mathbf{1}'^* = \mathbf{1}$ and $\mathbf{1}'' \times \mathbf{1}''^* = \mathbf{1}$. This is the reason to assign L_i and l_i the same representation, to maintain the charged lepton masses diagonal. The Majorana masses for the right-handed neutrinos are obtained from the terms proportional to M_4, M_5, M, M_{45}, and after A_4 breaking from the Yukawa couplings of ϕ. The Dirac mass terms for neutrinos are obtained from the Yukawa couplings of η with L_i and N_T and from the couplings of H and L_i with N_4 and N_5. The resultant Dirac and right-handed Majorana mass matrices, m_D and M_R respectively, are then used to obtain the light neutrino mass matrix through the type-I seesaw mechanism. The light neutrino mass matrix is then

$$m_\nu = -m_D M_R^- 1 m_D^T. \tag{4.17}$$

We will concentrate on models with a remnant Z_2 symmetry. This is phenomenologically interesting because a remnant Z_2 stabilizes the lightest particle odd under it, in this case it can either be a scalar or a fermion. This lightest Z_2 odd particle is a candidate for Dark Matter.
Given the matter content in table (4.2) we obtain different light neutrino mass matrix textures using different assignments of α, β, γ and ε. We obtain the correspondence between irreps assignment and neutrino textures as shown in Table (4.3). This work is focused on the models for A_1 and A_2 because they lead to the interesting case of non-observable neutrinoless double beta decay, they contain dark matter candidates and because these textures are statistically favored over the others [37].

L_e	$L_m u$	L_τ	N_4	N_5	Matrix Texture
1	$1''$	$1'$	1	$1'$	B_3
1	$1''$	$1'$	1	$1''$	B_4
$1''$	1	$1'$	1	$1'$	A_1
$1''$	$1'$	1	1	$1'$	A_2

Table 4.3: Particle representations under A_4 symmetry giving rise to different neutrino mass matrix textures. The nomenclature of the matrices follow [38].

4.3.2 Model for A_1 texture

To obtain an A_1 texture we assign the following representations

$$\alpha = \mathbf{1}'', \beta = \mathbf{1}, \gamma = \mathbf{1}', \delta = \mathbf{1}, \varepsilon = \mathbf{1}'. \tag{4.18}$$

The Lagrangian for this model is then

$$\begin{aligned} \mathscr{L}_Y &= y_e \overline{L}_e l_e H + y_\mu \overline{L}_\mu l_\mu H + y_\mu \overline{L}_\mu l_\mu H \\ &+ y_1^\nu \overline{L}_e \left[N_T \eta\right]_{1''} + y_2^\nu \overline{L}_\mu \left[N_T \eta\right]_1 + y_3^\nu \overline{L}_\tau \left[N_T \eta\right]_{1'} \\ &+ y_4^{\nu 2} \overline{L}_\mu N_4 H + y_5^{\nu 3} \overline{L}_\tau N_5 H + M \overline{N_T^c} N_T \\ &+ M_4 N_4^c N_4 + y_2^{N_1} \left[\overline{N_T^c} \phi\right]_1 N_4 + y_3^{N_{1'}} \left[\overline{N_T^c} \phi\right]_{1''} N_5 \\ &+ y_1^N \left[\overline{N_T^c} \phi\right]_3 N_T + (y_1^N)' \left[\overline{N_T^c} \phi\right]_{3_2} N_T + h.c. \quad . \end{aligned} \tag{4.19}$$

To obtain neutrino masses the scalar fields develop the following vevs

$$\langle H \rangle = (0, v_H)^T, \langle \eta \rangle = (0, \overline{v_\eta})^T, \langle \phi \rangle = \overline{v_\phi} \tag{4.20}$$

in EW space and

$$\overline{v_\eta} = (v_\eta, 0, 0), \overline{v_\phi} = (v_\phi, 0, 0) \tag{4.21}$$

in flavor space. This form of the vevs in EW space ensures the breaking of $SU(2)_L \times U(1)_Y$ to $U(1)_{EM}$ as in the Standard Model. The form of the vevs in flavor space ensures that the remnant symmetry is Z_2. The only fields odd under this Z_2 are $\phi_{2,3}$, $\eta_{2,3}$ and $N_{2,3}$.
After the breaking of these symmetries we obtain the right-handed neutrino Majorana mass matrix

$$M_R = \begin{pmatrix} M & 0 & 0 & v_\phi y_2^{N_1} & v_\phi y_3^{N_{1'}} \\ 0 & M & M_\phi & 0 & 0 \\ 0 & M_\phi & M & 0 & 0 \\ v_\phi y_2^{N_1} & 0 & 0 & M_4 & 0 \\ v_\phi y_3^{N_{1'}} & 0 & 0 & 0 & 0 \end{pmatrix}, \tag{4.22}$$

where $M_\phi = v_\phi(y_1^N + (y_1^N)')$. The Dirac mass matrix takes the form

$$m_D = \begin{pmatrix} v_\eta y_1^\nu & 0 & 0 & 0 & 0 \\ v_\eta y_2^\nu & 0 & 0 & v_H y_4^{\nu 2} & 0 \\ v_\eta y_3^\nu & 0 & 0 & 0 & v_H y_5^{\nu 3} \end{pmatrix}. \tag{4.23}$$

The resultant light neutrino mass matrix is obtained with the type-I seesaw formula (4.17), and is as follows

$$m_\nu = \begin{pmatrix} 0 & 0 & w \\ 0 & x & y \\ w & y & z \end{pmatrix}, \tag{4.24}$$

where

$$\begin{aligned} w &= \frac{-v_H v_\eta y_1^\nu y_5^{\nu 3}}{(v_\phi y_3^{N_{1'}})}, \\ x &= \frac{-v_H^2 (y_4^{\nu 2})^2}{M_4}, \\ y &= \frac{y_3^{N_{1'}} v_H (v_H v_\phi y_4^{\nu 2} y_2^{N_1} - v_\eta M_4 y_2^\nu)}{M_4 v_\phi y_3^{N_{1'}}}, \\ z &= \frac{y_3^{N_{1'}} v_H (M M_4 y_3^{N_{1'}} v_H - 2 M_4 y_3^\nu y_3^{N_{1'}} v_\phi v_\eta - v_H v_\phi^2 (y_2^{N_1})^2 y_3^{N_{1'}})}{M_4 v_\phi^2 (y_3^{N_{1'}})^2}. \end{aligned} \tag{4.25}$$

. This matrix has the form of the A_1 texture as classified in [38]. An immediate consequence of a zero in the m_{ee} entry is the unobservability of the neutrinoless double beta decay, despite of the fact that neutrinos are Majorana particles in the model and thus violate lepton number by two units.

4.3.3 Model for A_2 texture

In this instance we need the representations

$$\alpha = \mathbf{1}'', \beta = \mathbf{1}', \gamma = \mathbf{1}, \delta = \mathbf{1}, \varepsilon = \mathbf{1}', \tag{4.26}$$

as defined before, yielding the Lagrangian

$$\begin{aligned} \mathscr{L}_Y &= y_e \overline{L}_e l_e H + y_\mu \overline{L}_\mu l_\mu H + y_\mu \overline{L}_\mu l_\mu H \\ &+ y_1^\nu \overline{L}_e [N_T \eta]_{1''} + y_2^\nu \overline{L}_\mu [N_T \eta]_{1'} + y_3^\nu \overline{L}_\tau [N_T \eta]_1 \\ &+ y_4^{\nu 3} \overline{L}_\tau N_4 H + y_5^{\nu 1} \delta_{\alpha\delta} \overline{L}_e N_5 H + M \overline{N_T^c} N_T \\ &+ M_5 \overline{N_5^c} N_5 + y_2^{N_1} \left[\overline{N_T^c} \phi\right]_1 N_4 + y_3^{N_{1''}} \left[\overline{N_T^c} \phi\right]_{1''} N_5 \\ &+ y_1^N \left[\overline{N_T^c} \phi\right]_{3_1} N_T + (y_1^N)' \left[\overline{N_T^c} \phi\right]_{3_2} N_T + h.c. \quad . \end{aligned} \tag{4.27}$$

(4.28)

After EW and A_4 symmetry breaking we obtain the same right-handed neutrino Majorana mass matrix as in eq.(4.22), but the Dirac mass matrix is now

$$m_D = \begin{pmatrix} v_\eta y_1^\nu & 0 & 0 & 0 & 0 \\ v_\eta y_2^\nu & 0 & 0 & 0 & v_H y_5^{\nu 2} \\ v_\eta y_3^\nu & 0 & 0 & v_H y_4^{\nu 3} & 0 \end{pmatrix}. \tag{4.29}$$

The resulting light neutrino mass matrix is

$$m_\nu = \begin{pmatrix} 0 & w' & 0 \\ w' & x' & y' \\ 0 & y' & z' \end{pmatrix}, \tag{4.30}$$

where

$$\begin{aligned} w' &= \frac{-v_H v_\eta y_5^{\nu 2} y_1^\nu}{v_\phi y_3^{N_{1'}}}, \\ x' &= \frac{v_H y_5^{\nu 2}(-2M_4 v_\eta v_\phi y_2^\nu y_3^{N_{1'}} + M M_4 v_H y_5^{\nu 2} - v_H v_\phi^2 (y_2^{N_1})^2 y_5^{\nu 2})}{M_4 v_\phi^2 (y_3^{N_{1'}})^2}, \\ y' &= \frac{v_H(-M_4 v_\eta y_3^\nu + v_H v_\phi y_2^{N_1} y_4^{\nu 3}) y_5^{\nu 2}}{M_4 v_\phi y_3^{N_{1'}}}, \\ z' &= \frac{-v_h^2 (y_4^{\nu 3})^2}{M_4}. \end{aligned} \tag{4.31}$$

This is the A_2 texture, in the classification defined by (REF). As in the last model the entry m_{ee} of the matrix is zero, resulting in unobservable neutrinoless double beta decay.

4.3.4 Other models

As reported in [39], the framework presented here is capable of generating models for the B_3 and B_4 matrix textures when the lepton doublets and right-handed neutrinos are assigned the A_4 irreps shown in Table (4.3). In these models a remnant Z_2 can be obtained as well, leading to the presence of a dark matter candidate. In contrast to the A_1 and A_2 textures, however, the m_{ee} entry of the neutrino mass matrix is nonzero at tree level, leading to observable neutrinoless double beta decay. Additionally the B_1 and B_2 textures can be obtained by expanding the model with a scalar $SU(2)_L$ triplet . Obtaining these textures requires breaking A_4 to Z_3, charging under the residual symmetry the charged leptons, excluding the existence of a dark matter candidate.

4.3.5 Model Phenomenology

We focus on the models for A_1 and A_2 for the following reasons. The zero entry of m_{ee} implies unobservable neutrinoless double beta decay, making the determination of the Majorana nature of neutrinos impossible through this observable, widely considered to be the golden standard for this. In addition to this, as pointed out in [37], the A_1 and A_2 textures are less constrained by the observed values of mixing angles and squared mass differences, without conflicting with cosmological bounds on neutrino masses. The phenomenology of the two zero texture neutrino matrices has been extensively studied [38, 40, 41], here we The resulting light neutrino mass matrices m_ν are related to the neutrino mixing matrix U_{MNSP} and the complex neutrino mass matrix in the mass basis $diag(\mu_1, \mu_2, \mu_3)$ with the equation

$$m_\nu = U_{MNSP} diag(\mu_1, \mu_2, \mu_3) U_{MNSP}^T. \tag{4.32}$$

We adopt the convention where the physical Majorana phases are located in μ_2 and μ_3, that is to say,

$$\mu_1 = m_1 \in \mathbb{R} \quad , \quad \mu_{2,3} = \mathrm{m}_{2,3} \mathrm{e}^{\mathrm{i}\alpha_{2,3}}, \quad \mathrm{m}_{2,3} \in \mathbb{R}. \tag{4.33}$$

The two independent zeros in m_ν then relate the masses and mixing angles in the following manner

$$\begin{aligned} \mu_2 &= \left(1 + \frac{sin\theta_{23}}{cos\theta_{12}cos\theta_{23}sin\theta_{12}sin\theta_{13}e^{-i\delta} - sin^2\theta_{12}sin\theta_{23}}\right)\mu_1 \\ \mu_3 &= \pm\left(\frac{-cot\theta_{13}cos\theta_{12}cos\theta_{23}e^{2i\delta}}{cos\theta_{12}cos\theta_{23}sin\theta_{13} - sin\theta_{12}sin\theta_{23}e^{i\delta}}\right)\mu_1. \end{aligned} \tag{4.34}$$

We can approximate these relationships taking into account the smallness of θ_{13} by neglecting $sin\theta_{13}$ terms obtaining

$$\mu_2 = -\mu_1 cot^2\theta_{12} \quad , \quad \mu_3 = \pm\mu_1 e^{i\delta}\frac{cot\theta_{12}cot\theta_{23}}{sin\theta_{13}}. \tag{4.35}$$

All predictions derived from these equation receive small corrections from the observed nonzero value of θ_{13}.
From the measured values of the mixing angles and squared mass differences the inverse hierarchy is excluded. This is because

$$cot^2\theta_{12} \sim 3, \tag{4.36}$$

which implies

$$m_2 > m_1. \tag{4.37}$$

Using the normal hierarchy values for the oscillation parameters, the allowed range of values for the lightest neutrino mass m_1 are

$$A_1: \quad m1 \in [4,8]meV \tag{4.38}$$
$$A_2: \quad m1 \in [3,8]meV. \tag{4.39}$$

We can also immediately extract the approximate values of the Majorana phases from 4.35

$$A_1: \quad \alpha_2 = \pi \quad , \quad \alpha_3 = \delta, \tag{4.40}$$
$$A_2: \quad \alpha_2 = \pi \quad , \quad \alpha_3 = \delta + \pi. \tag{4.41}$$

The zeros of the neutrino mixing matrices are not protected to all orders of perturbation, in fact they receive contributions at one loop order. The responsible diagram is shown in Fig (4.1). For each model a rough approximation to the value of this correction can be obtained by considering the largest entry in the matrix with the same Yukawa coupling as the neutrinos in the zero entry, and multiplying by the usual $(4\pi)^{-2}$ one loop factor. The values of the nonzero entries are restricted by the equation (4.32), together with the oscillation parameters and the cosmological neutrino mass limit. The resulting estimations for the correction of the most stringently constrained observable, m_{ee} are

$$m_{ee} \sim 8 \times 10^{-5} eV \tag{4.42}$$

for both textures. The current limit on this matrix element is 0.2 eV and the projected sensitivity of near-future experiments is 0.01 eV [34].

4.3.6 Dark Matter stability

As mentioned before, the remnant Z_2 defines a dark sector, which is composed of $N_{2,3}, \phi_{2,3}, \eta_{2,3}$. Under this Z_2 these fields transform as

$$N_2 \to -N_2 \quad , \quad \eta_2 \to -\eta_2 \quad , \quad \phi_2 \to -\phi_2, \tag{4.43}$$
$$N_3 \to -N_3 \quad , \quad \eta_3 \to -\eta_3 \quad , \quad \phi_3 \to -\phi_3. \tag{4.44}$$

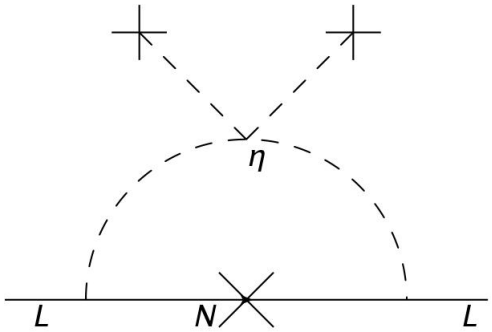

Figure 4.1: Feynman diagram of the models giving rise to nonzero m_{ee}.

Generically, these fields will mix among themselves, respecting Lorentz invariance, and will produce a set of 2 fermion and 4 scalar dark mass eigenstates. These eigenstates will transform as odd under Z_2 as well. The lightest particle in the dark sector will be a candidate for dark matter. The dark matter phenomenology can be divided in two cases, the scalar and the fermion case. In the scalar case the dark matter phenomenology will be somewhat similar to an Inert Singlet Higgs Model,if the lightest dark particle is primarily ϕ, or to the Inert Higgs Doublet Model otherwise, as analyzed in [42] . In the fermion case the phenomenology can be characterized as a Majorana dark matter with a scalar portal to the SM, very similar to the Scotogenic Model [43], but with the addition of an annihilation channel for dark matter, which can alleviate the tension between LFV observables and the freeze-out mechanism inherent to the Scotogenic.

4.3.7 A_1 texture phenomenology

The A_1 texture is defined by the zeros in the m_{ee} and $m_{\mu\mu}$. The immediate constraints from these zeros are

$$cos^2\theta_{12}cos^2\theta_{13}\mu_1 + cos^2\theta_{13}sin^2\theta_{12}\mu_2 + e^{-2i\delta}sin^2\theta_{13}\mu_3 = 0 \tag{4.45}$$
$$(-cos\theta_{12}cos\theta_{13}cos\theta_{23}sin\theta_{12} - cos\theta_{13}e^{i\delta}sin\theta_{13}sin\theta_{23} + cos\theta_{13}e^{(i\delta)}sin^2\theta_{12}sin\theta_{13}sin\theta_{23})\mu_1 +$$
$$(cos\theta_{12}cos\theta_{13}cos\theta_{23}sin\theta_{12} - cos\theta_{13}e^{(i\delta)}sin^2\theta_{12}sin\theta_{13}sin\theta_{23})\mu_2 +$$
$$cos\theta_{13}e^{-i\delta}sin\theta_{13}sin\theta_{23}\mu_3 = 0,$$

which can be reduced to constraints on μ_2 and μ_3

$$\mu_2 = \left(1 + \frac{sin\theta_{23}}{cos\theta_{12}cos\theta_{23}sin\theta_{12}sin\theta_{13}e^{-i\delta} - sin^2\theta_{12}sin\theta_{23}}\right)\mu_1$$
$$\mu_3 = \left(\frac{-cot\theta_{13}cos\theta_{12}cos\theta_{23}e^{2i\delta}}{cos\theta_{12}cos\theta_{23}sin\theta_{13} - sin\theta_{12}sin\theta_{23}e^{i\delta}}\right)\mu_1. \quad (4.46)$$

For $m_{ee} = 0$ an inverted hierarchy neutrino spectrum is excluded. Using the measured oscillation parameters [18], a scan is performed to obtain predictions for δ, m_1, and the Majorana phases α_2 and α_3. The results are shown in Figure (4.2). From these numerical scan we see that the Dirac phase δ is predicted to be in the range $[0.8 - 1.7]\pi$. The Majorana phase α_2 lies near π, receiving corrections from nonzero θ_{13}. The remaining phase α_3 depends strongly on the value of δ, preferring values between π and 2π.

4.3.8 A_2 texture phenomenology

The A_2 is defined by zeros in the entries m_{ee} and $m_{e\tau}$. The resulting constraints are

$$\mu_2 = \left(1 - \frac{cos\theta_{23}}{sin\theta_{12}sin\theta_{23}cos\theta_{12}sin\theta_{13}e^{-i\delta} + sin^2\theta_{12}cos\theta_{23}}\right)\mu_1$$
$$\mu_3 = \left(\frac{-cot\theta_{13}cos\theta_{12}sin\theta_{23}e^{2i\delta}}{cos\theta_{12}sin\theta_{23}sin\theta_{13} + sin\theta_{12}cos\theta_{23}e^{i\delta}}\right)\mu_1. \quad (4.47)$$

As in the first texture, we perform a scan over the fitted values of the oscillation parameters from [18]. The results are shown in Figure (4.3). The values for δ in this case can reach 2π and a little beyond up to 0.1π. In contrast to the last case, the corrections from nonzero θ_{13} move the value of α_2 from π to values below π. As in the last case, α_3 depends strongly on δ.

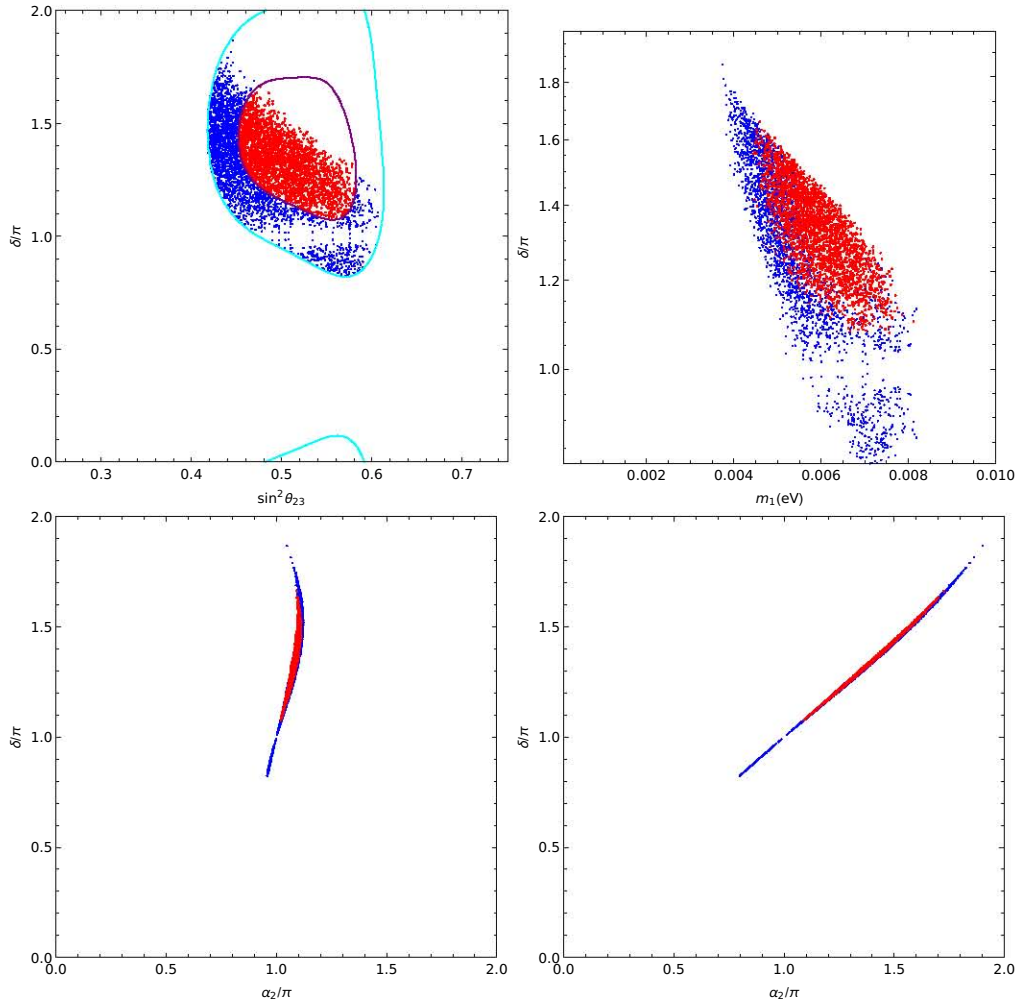

Figure 4.2: Results for the numerical scan of the A_1 texture using the oscillation parameters at 3σ(blue points) and 1σ (red points) C.L.The upper left panel shows the correlation between the $sin^2\theta_{23}$ and the Dirac CP violating phase δ. The contours represent the 3σ (light blue) and 1σ (red) C.L. from NuFit [18]. The upper right panel shows the allowed values of the lightest neutrino mass as function of δ, showing the range $[3-8]$meV as favored by this texture. The lower left and right panels show the correlations between δ and the Majorana phases α_2 and α_3 respectively. The α_2 phase lies very near the middle point Π. The α_3 phase is strongly correlated with δ.

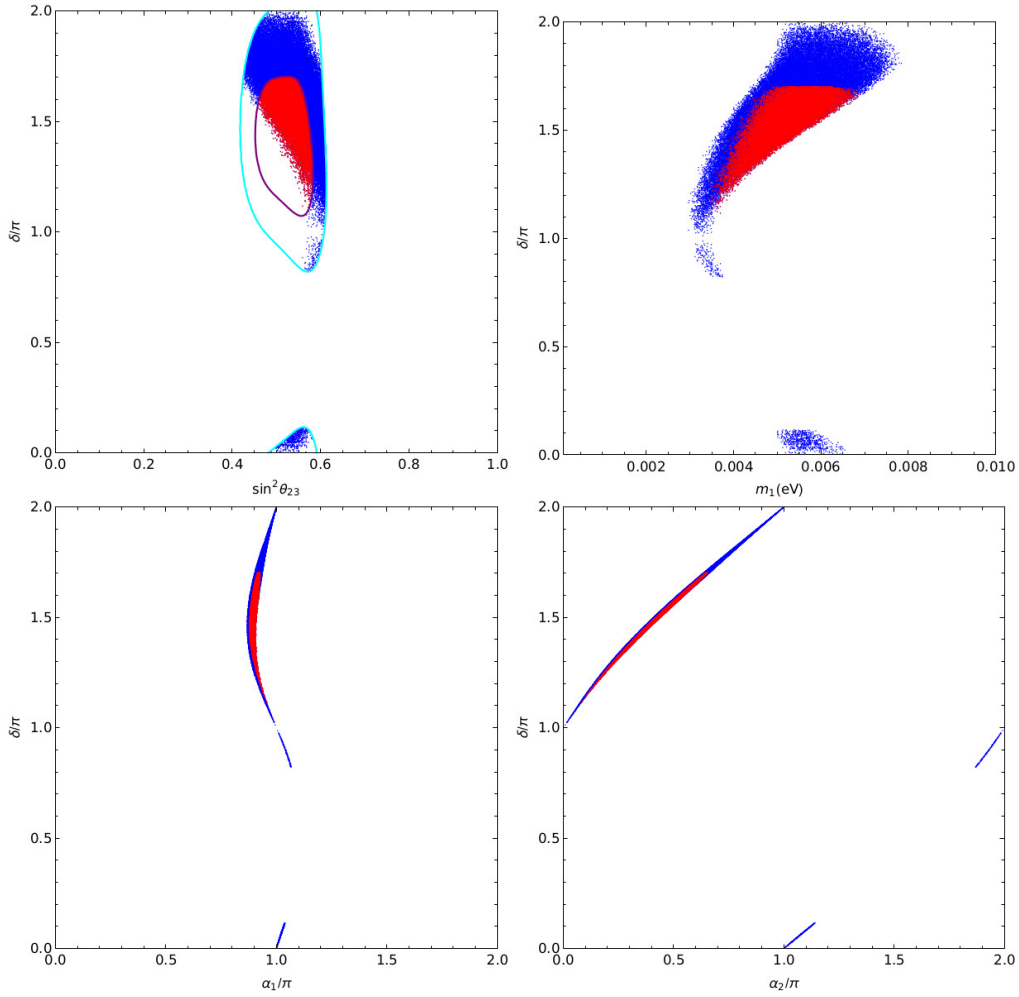

Figure 4.3: Results for the numerical scan of the A_2 texture using the oscillation parameters at 3σ(blue points) and 1σ (red points) C.L.The upper left panel shows the correlation between the $sin^2\theta_{23}$ and the Dirac CP violating phase δ. The contours represent the 3σ (light blue) and 1σ (red) C.L. from NuFit [18]. The upper right panel shows the allowed values of the lightest neutrino mass as function of δ, showing the range $[3-8]$meV as favored by this texture. The lower left and right panels show the correlations between δ and the Majorana phases α_2 and α_3 respectively. The α_2 phase lies very near the middle point Π. The α_3 phase is strongly correlated with δ.

Chapter 5

Conclusion

In this work we have briefly reviewed basic mechanisms for the generation of Majorana masses and flavor symmetries. We have applied this to an A_4 symmetric model, which after the flavor symmetry breaking generates viable Majorana neutrino masses and leaves a Z_2 symmetry behind. The Z_2 symmetry defines a dark sector with a stable dark matter candidate. The flavor symmetry generates zeroes in the neutrino mass matrix, which result in correlations between the masses and mixing angles. We analysed the phenomenology and viability of these matrix textures and focused on a pair of them, A_1 and A_2, where neutrinoless double beta decay is unobservable. Additionally the flavor symmetry predicts nonzero Dirac and Majorana phases, introducing sizable CP violation to the lepton sector. Although the dark sector remains unexplored, the particle content and symmetry suggests a strong similarity to existing models, namely to the inert scalar models, which have been extensively studied before and remain viable for heavy ($>\sim 500$ GeV) dark matter masses. The consequences for the models considered are important, since neutrinoless double beta decay is the most sensitive avenue for the observation of $|\Delta L| = 2$ processes. If neutrinoless double beta decay is unobservable, the determination of the Majorana nature of neutrinos would be theoretically possible with other less sensitive processes only, like lepton flavor violating decays of mesons, which are sensitive to the nonzero elements of the neutrino mass matrix. In summary, the addition of a flavor symmetry to the SM, with right-handed neutrinos and scalar fields can result in the generation of phenomenologically viable neutrino Majorana mass matrices and a dark sector with a stable dark matter candidate.

Bibliography

[1] F. Zwicky. Die Rotverschiebung von extragalaktischen Nebeln. Helvetica Physica Acta, 6:110–127, 1933.

[2] Heinz Andernach and Fritz Zwicky. English and Spanish Translation of Zwicky's (1933) The Redshift of Extragalactic Nebulae. arXiv e-prints, page arXiv:1711.01693, Nov 2017.

[3] V. C. Rubin, N. Thonnard, and W. K. Ford, Jr. Rotational properties of 21 SC galaxies with a large range of luminosities and radii, from NGC 4605 /R = 4kpc/ to UGC 2885 /R = 122 kpc/. Astrophys. J., 238:471, 1980.

[4] Maxim Markevitch, A. H. Gonzalez, D. Clowe, A. Vikhlinin, L. David, W. Forman, C. Jones, S. Murray, and W. Tucker. Direct constraints on the dark matter self-interaction cross-section from the merging galaxy cluster 1E0657-56. Astrophys. J., 606:819–824, 2004.

[5] Stefano Profumo. An Introduction to Particle Dark Matter. World Scientific, 2017.

[6] M. Milgrom. A modification of the Newtonian dynamics as a possible alternative to the hidden mass hypothesis. , 270:365–370, July 1983.

[7] Anze Slosar, Alessandro Melchiorri, and Joseph Silk. Did Boomerang hit MOND? Phys. Rev., D72:101301, 2005.

[8] Douglas Clowe, Marusa Bradac, Anthony H. Gonzalez, Maxim Markevitch, Scott W. Randall, Christine Jones, and Dennis Zaritsky. A direct empirical proof of the existence of dark matter. Astrophys. J., 648:L109–L113, 2006.

[9] B. Pontecorvo. Inverse beta processes and nonconservation of lepton charge. Sov. Phys. JETP, 7:172–173, 1958. [Zh. Eksp. Teor. Fiz.34,247(1957)].

[10] Samoil M. Bilenky. Neutrino oscillations: brief history and present status. In Proceedings, 22nd International Baldin Seminar on High Energy Physics Problems, Relativistic Nuclear Physics and Quantum Chromodynamics, (ISHEPP 2014): Dubna, Russia, September 15-20, 2014, 2014.

[11] Q. R. Ahmad et al. Direct evidence for neutrino flavor transformation from neutral current interactions in the Sudbury Neutrino Observatory. Phys. Rev. Lett., 89:011301, 2002.

[12] Y. Fukuda et al. Evidence for oscillation of atmospheric neutrinos. Phys. Rev. Lett., 81:1562–1567, 1998.

[13] Paul Langacker. The standard model and beyond. 2010.

[14] M. Tanabashi et al. Review of Particle Physics. Phys. Rev., D98(3):030001, 2018.

[15] M. E. Shaposhnikov. Baryon Asymmetry of the Universe in Standard Electroweak Theory. Nucl. Phys., B287:757–775, 1987.

[16] K. Moffat, S. Pascoli, S. T. Petcov, and J. Turner. Leptogenesis from Low Energy *CP* Violation. JHEP, 03:034, 2019.

[17] Ettore Majorana. Teoria simmetrica dell'elettrone e del positrone. Il Nuovo Cimento (1924-1942), 14(4):171, Sep 2008.

[18] Ivan Esteban, M. C. Gonzalez-Garcia, Michele Maltoni, Ivan Martinez-Soler, and Thomas Schwetz. Updated fit to three neutrino mixing: exploring the accelerator-reactor complementarity. JHEP, 01:087, 2017.

[19] V. N. Aseev et al. An upper limit on electron antineutrino mass from Troitsk experiment. Phys. Rev., D84:112003, 2011.

[20] Ch. Kraus et al. Final results from phase II of the Mainz neutrino mass search in tritium beta decay. Eur. Phys. J., C40:447–468, 2005.

[21] N. Aghanim et al. Planck 2018 results. VI. Cosmological parameters. 2018.

[22] J. Schechter and J. W. F. Valle. Neutrino masses in su(2) $\otimes$ u(1) theories. Phys. Rev. D, 22:2227–2235, Nov 1980.

[23] Steven Weinberg. Baryon- and lepton-nonconserving processes. Phys. Rev. Lett., 43:1566–1570, Nov 1979.

[24] Murray Gell-Mann, Pierre Ramond, and Richard Slansky. Complex Spinors and Unified Theories. Conf. Proc., C790927:315–321, 1979.

[25] Peter Minkowski. $\mu \to e\gamma$ at a Rate of One Out of 10^9 Muon Decays? Phys. Lett., 67B:421–428, 1977.

[26] Tsutomu Yanagida. Horizontal gauge symmetry and masses of neutrinos. Conf. Proc., C7902131:95–99, 1979.

[27] Rabindra N. Mohapatra and Goran Senjanovic. Neutrino Masses and Mixings in Gauge Models with Spontaneous Parity Violation. Phys. Rev., D23:165, 1981.

[28] R. Foot, H. Lew, X. G. He, and G. C. Joshi. See-saw neutrino masses induced by a triplet of leptons. Zeitschrift für Physik C Particles and Fields, 44(3):441–444, Sep 1989.

[29] J. D. Vergados. Neutrinoless Double Beta Decay Without Majorana Neutrinos in Supersymmetric Theories. Phys. Lett., B184:55–62, 1987.

[30] J. Schechter and J. W. F. Valle. Neutrinoless Double beta Decay in SU(2) x U(1) Theories. Phys. Rev., D25:2951, 1982. [,289(1981)].

[31] Michael Duerr, Manfred Lindner, and Alexander Merle. On the Quantitative Impact of the Schechter-Valle Theorem. JHEP, 06:091, 2011.

[32] A. Gando et al. Search for Majorana Neutrinos near the Inverted Mass Hierarchy Region with KamLAND-Zen. Phys. Rev. Lett., 117(8):082503, 2016. [Addendum: Phys. Rev. Lett.117,no.10,109903(2016)].

[33] Jonathan Engel and Javier Menéndez. Status and Future of Nuclear Matrix Elements for Neutrinoless Double-Beta Decay: A Review. Rept. Prog. Phys., 80(4):046301, 2017.

[34] Michelle J. Dolinski, Alan W. P. Poon, and Werner Rodejohann. Neutrinoless Double-Beta Decay: Status and Prospects. Submitted to: Ann. Rev. Nucl. Part. Phys., 2019.

[35] Alexander Dueck, Werner Rodejohann, and Kai Zuber. Neutrinoless double beta decay, the inverted hierarchy and precision determination of theta(12). Physical Review D - PHYS REV D, 83, 03 2011.

[36] J. Kubo, A. Mondragon, M. Mondragon, and E. Rodriguez-Jauregui. The Flavor symmetry. Prog. Theor. Phys., 109:795–807, 2003. [Erratum: Prog. Theor. Phys.114,287(2005)].

[37] Julien Alcaide, Jordi Salvado, and Arcadi Santamaria. Fitting flavour symmetries: the case of two-zero neutrino mass textures. JHEP, 07:164, 2018.

[38] Paul H. Frampton, Sheldon L. Glashow, and Danny Marfatia. Zeroes of the neutrino mass matrix. Phys. Lett., B536:79–82, 2002.

[39] J. M. Lamprea and E. Peinado. Seesaw scale discrete dark matter and two-zero texture Majorana neutrino mass matrices. Phys. Rev., D94(5):055007, 2016.

[40] Walter Grimus, Anjan S. Joshipura, Luis Lavoura, and Morimitsu Tanimoto. Symmetry realization of texture zeros. Eur. Phys. J., C36:227–232, 2004.

[41] M. Hirsch, Anjan S. Joshipura, S. Kaneko, and J. W. F. Valle. Predictive flavour symmetries of the neutrino mass matrix. Phys. Rev. Lett., 99:15Desarrollo de la propuesta de investigación., 2007.

[42] M. S. Boucenna, M. Hirsch, S. Morisi, E. Peinado, M. Taoso, and J. W. F. Valle. Phenomenology of Dark Matter from A_4 Flavor Symmetry. JHEP, 05:037, 2011.

[43] Ernest Ma. Verifiable radiative seesaw mechanism of neutrino mass and dark matter. Phys. Rev., D73:077301, 2006.